Proceedings of the ASME 2020
International Design Engineering Technical Conferences
and Computers and Information in Engineering Conference
IDETC/CIE2020
August 17-19, 2020, Virtual, Online

DETC2020-22049

HINGES AND CURVED LAMINA EMERGENT TORSIONAL JOINTS IN CYLINDRICAL DEVELOPABLE MECHANISMS

Kendall Seymour
Dept. of Mechanical Engineering
Brigham Young University
Provo, Utah 84602
Email: kennyseymour@byu.edu

Pietro Bilancia*
Dept. of Mechanical, Energy, Management
and Transportation Engineering
University of Genova
Genova, Italy 16145
Email: pietro.bilancia@edu.unige.it

Spencer Magleby
Dept. of Mechanical Engineering
Brigham Young University
Provo, Utah 84602
Email: magleby@byu.edu

Larry Howell
Dept. of Mechanical Engineering
Brigham Young University
Provo, Utah 84602
Email: lhowell@byu.edu

ABSTRACT

Cylindrical developable mechanisms are devices that conform to and emerge from a cylindrical surface. These mechanisms can be formed or cut from the cylinder wall itself. This paper presents a study on adapting traditional hinge options to achieve revolute motion in these mechanisms. A brief overview of options is given, including classical pin hinges, small-length flexural pivots, initially curved beams, and an adaptation of the membrane thickness-accommodation technique. Curved Lamina Emergent Torsional (LET) joints are then evaluated in detail, and a thin-walled modeling assumption is checked analytically and empirically. A small-scale cylindrical developable mechanism is then evaluated with Nitinol curved LET joints.

1 INTRODUCTION

Developable mechanisms (DMs) are mechanisms that conform to and emerge from developable surfaces [1, 2]. These surfaces can be formed from a flat sheet without stretching or tearing the material, and a straight line can be fit to the surface at any point. Developable surfaces are of interest because they represent a large range of surfaces seen in manufactured finished products and can be mathematically modeled using relatively simple models [2]. DMs have the unique ability to be made or cut from the same material as the developable surface, in the way that lamina emergent mechanisms (LEMs) [3] are cut from planar materials.

Cylindrical DMs [4] conform to or emerge from a cylindrical surface. Laparoscopic surgical tools, which are usually cylindrical [5–8], are being scaled down to reach smaller and more restrictive spaces in the body [9, 10]. Therefore, the simplistic design and conforming nature of these mechanisms show potential for impact in industries such as the medical field where small-scale tooling is used [7]. At the laparoscopic surgical scale, where cylindrical shafts can be 3 mm in diameter, design becomes difficult due to the nature of manufacturing, part assembly, low gripping forces, and relatively high friction forces [11]. These difficulties can be addressed through compliant mechanisms [12], which can have much lower part counts, are more scalable than traditional pin and link mechanisms, and reduce

*Address all correspondence to this author.

friction. The traits of DMs could facilitate small-scale, compliant, and potentially monolithic cylindrical mechanisms. Preliminary research on DMs has focused on the theory behind their motion and a few potential applications [2, 4, 13]. These studies operated under the assumption that revolute joints exist between the rigid links. Therefore, joint options for DMs on cylinders are needed to enable these mechanisms to take a physical and practical form.

This paper presents design considerations and resources for modeling hinges in cylindrical DMs. The rest of the paper is organized as follows: Section 2 gives background information necessary to understand the topics and theory discussed in the paper, Section 3 reports a top-level analysis of potential joint designs for cylindrical DMs, Section 4 reviews analytical, numerical and physical testing work performed to check thin-walled approximation for curved lamina emergent torsional (LET) joints, Section 5 demonstrates the potential for LET joints in cylinders by briefly reviewing a demonstrative small-scale cylindrical DM with Nitinol LET joints modeled with finite element analysis (FEA), whereas Section 6 summarizes the concluding remarks.

2 BACKGROUND

2.1 Cylindrical Developable Mechanisms

Developable surfaces are smooth surfaces with a zero Gaussian curvature, or curvature in only one direction with the perpendicular direction being flat. These surfaces can be folded flat without stretching or tearing the surface. The orientation of the ruling lines, or lines that can be fit to the surface at any point, defines the type of developable surface. The three non-trivial developable surfaces are generalized cylinders, generalized cones, and tangent developed surfaces, as shown in [1]. A DM can be created from any developable surface by aligning the hinge axes of a specific kinematic mechanism with the ruling lines of the surface [1]. An example of cylindrical DM [4] is shown in Fig. 1. While LEMs are formed into planar surfaces, DMs allow kinematic mechanisms to exist on or in curved shapes. Cylindrical DMs have a wide range of applications in research and industry, such as curved train and airplane doors with smooth integration and simple actuation, wheels with an embedded mechanism to enable a walking motion, or emergency medical devices that quickly secure themselves to the body.

2.2 Compliant and Lamina Emergent Mechanisms

A compliant mechanism gains mobility through the flexibility of its members [12]. The development of various analysis techniques have enabled compliant mechanisms to be customized for many applications and become prevalent in many industries [14–17]. LEMs are planar compliant mechanisms often cut from sheet material that emerge out of plane as they actuate. Planar micromachining processes have enabled micro- and nano-scale LEM devices to be designed and analyzed [18, 19]. However, only change-point mechanisms can be made into LEMs due to their initial flat state [3]. LEMs have been adapted to create hinge-like motion along a desired axis in a planar material, resulting in the LET joints [20]. Arrays of these LET joints have been used to create developable surfaces from planar materials [21,22]. Curved LET joints were researched previously [23] and will be further explored in regards to their use in cylindrical DMs.

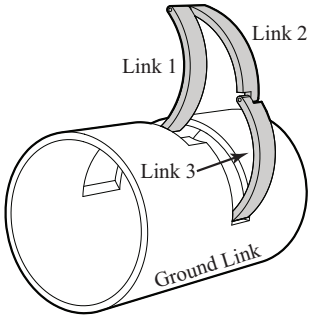

FIGURE 1. An example cylindrical DM. Links 1, 2, and 3 are highlighted, and the ground link is the cylinder body.

3 EVALUATION OF VARIOUS HINGE CANDIDATES

3.1 Joint Requirements

In many kinematic models, it is assumed that a revolute joint has the following characteristics:

1. No friction
2. No backlash
3. One rotational degree of freedom
4. A constant center of rotation
5. No energy storage

It is also assumed in kinematic models that rigid link lengths do not change throughout actuation, or the distances between joint axes of rotation do not change. While the properties of an ideal joint depend on the application, friction and backlash are generally undesirable, and a single degree of freedom per joint simplifies the actuation of the mechanism. Energy storage can be desirable in a mechanism, especially when attempting to create bistability through compliance [24]. For the purposes of this research, the ideal hinge for a cylindrical DM has no rubbing friction, no backlash, a single degree of freedom in rotation, and a constant center of rotation.

Previous work on cylindrical DMs [13] incorporated traditional pin joints during the prototyping phase. In the following, these classical methods of creating revolute joints are briefly discussed and their limitations given. Additional hinges and modeling options are then discussed, including small-length flexural pivots (SLFPs), initially curved cantilever beams, the membrane

fold technique, and curved LET joints. This leads to the next section, which shows a detailed analysis of thin-walled curved LET joints, including the adaptation of planar LET joint models to curved LET joints.

3.2 Classical Pin Joints

Pin hinges have been in use for centuries due to their simplicity and ease of manufacturing. They allow infinite rotation, disassembly of parts, and different material options between the pin and the links. However, the bearing surfaces often require lubrication, friction is inevitable, and there are issues when scaling to small sizes. Generally, the diameter of the pin needs to be less than the thickness of the link material. Therefore at small scales, such as those of laparoscopic surgical devices, direct shearing of the pin becomes a concern. For example, many laparoscopic devices are 5 mm in diameter with wall thicknesses about 0.5 mm or less [25]. A pin joint aligned with the ruling lines of the cylinder would need to have a diameter near 0.3 mm, or an area of 0.283 mm^2. At this dimension, a cylindrical pin made of 316 stainless steel would yield in direct shear with a load of only 87 N. Friction in these joints is also relatively high compared to the actuation force required, resulting in high energy losses between actuation and output force. Other kinematic joints, such as prismatic, spherical, and cylindrical joints could also be used to create cylindrical DMs, but they would share many of the same disadvantages as pin joints.

3.3 SLFPs and Initially Curved Cantilever Beams

SLFPs are areas of reduced stiffness in an otherwise rigid link that enable joint-like motion between rigid members [12, 26, 27]. If the reduced stiffness portion is significantly shorter and more flexible than the longer and more rigid portion, then a characteristic pivot, i.e. a location where a pin joint with a torsional spring can be used to model the behavior, is located in the center of the shorter, less-rigid portion. This modeling technique is termed the pseudo-rigid-body model (PRBM) [12] and is diagrammed in Fig. 2. With the PRBM, relatively simple equations can be used to model the rotation and end coordinates of the rigid portion given an input moment or forces. A closed-form elliptic integral solution for modeling initially curved SLFPs was previously developed [28]. Modeling an initially curved cantilever beam with the PRBM [29], as in Fig. 2, is a possible method that avoids using elliptic integrals.

However, there are three conditions present in a cylindrical DM with initially curved beam flexures that make modeling difficult or make the PRBM invalid for this case. First, when using the PRBM to model an initially curved cantilever beam, the characteristic pivot lies near the first 15% of the beam length, and is closer to the free end for higher curvature beams, as seen in Fig. 2. The pivot can also lie in space off the reference surface, or the developable surface used to create the DM. While this may

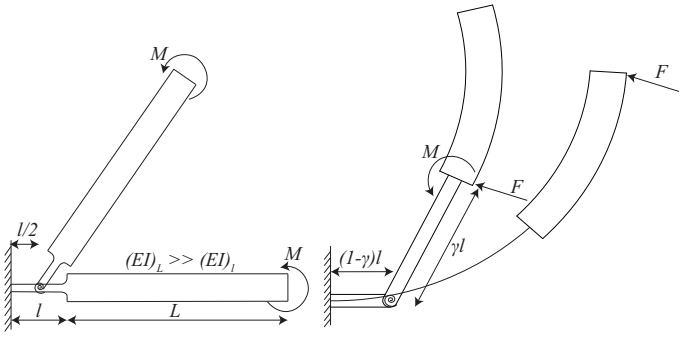

FIGURE 2. Left: PRBM for a SLFP. Right: PRBM for an initially-curved beam.

FIGURE 3. A 3D printed prototype of the expanding cylinder mechanism with one initially curved flexure, highlighted in white. The shape of the deflected flexure suggests it is loaded with end forces and moments, similar to a traditional fixed-guided beam.

enable new behaviors and features in DMs, it can also make kinematic modeling more difficult. If the characteristic pivot lies off the reference surface, the actual link length of the mechanism is different than the links of a DM with revolute joints that lie on the reference surface. Small changes in link lengths could alter the behavior and classification of the mechanism. Second, for initially curved beams that decrease their curvature during a mechanism's motion, the PRBM is only valid until the flexure reaches zero curvature, or a straight orientation [29]. Therefore, we must consider the deflected state of the mechanism and whether each initially curved flexure deflects in a direction that increases or decreases its curvature. This limits the use of this model to mechanisms that travel through relatively small deflections. The compliant link in the mechanism in Fig. 3 is at this deflection limit. The third difficulty arises when we consider the flexure's end conditions and loads. In the mechanism shown in Fig. 3, the right end of the white beam is guided through a non-conventional path, resulting in an end condition consisting of a force with changing magnitude and direction combined with a variable moment load. It can be seen in Fig. 3 that the pre-curved beam does not reach a flat state (which occurs with pre-curved beams with a pure moment on the end), but a shape more resembling a beam under fixed-guided end conditions.

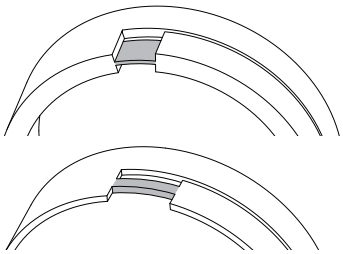

FIGURE 4. Top: The wall thickness reduction method (reduces h in beam) for creating SLFPs or pre-curved flexures. Bottom: The width reduction method (reduces w in beam), which is only viable when the cylinder wall thickness is less than the beam width.

In regards to manufacturing, there are two simple methods for reducing stiffness to create an SLFP or an initially curved cantilever beam to act as a joint: reduce either the width of the beam or the cylinder wall thickness in selected locations (see Fig. 4). Reducing the width of the beam can be done with many rotary manufacturing processes, such as a CNC machine or laser cutter. However, this method is only beneficial in thin-walled cylinders where the wall thickness is less than the width of the cut beam. It also does not aid in decreasing stress in the flexed member, as the depth of the beam in the direction of bending is not reduced. Decreasing cylinder wall thickness has opposing attributes. It is a more difficult manufacturing process, as small amounts of the cylinder wall need to be removed from inside or outside the cylinder, but it does aid in decreasing stress on the flexed member.

3.4 Membrane Technique

The membrane technique is one method for creating simple revolute motion and accommodating for thickness in origami designs [30, 31], and for reducing parasitic motion in LET joints [32]. In this technique, a thin flexible membrane is used to join the edges of rigid panels to create a relative folding motion. If the membrane holds the panels together while leaving a gap between panel edges, the folding and sandwiching of thick materials can be accomplished. The membrane may also exist on both sides of the panels and be significantly thicker than the panels themselves [33].

The membrane technique can be used to create hinge motion in cylindrical DMs, with some consideration. With thin-walled cylinders, the location of the membrane (whether is it attached to the inside or outside of the cylinder walls) affects the mechanism motion. This location is important to consider when using cylinders with considerable wall thickness, as the joints may then self-interfere and prevent the desired motion. However, prototyping efforts have revealed that for initially extramobile links, or links that move outward from the cylinder wall, the membrane should be applied to the outside of the cylinder, and vice versa for intramobile links. A prototype cylindrical parallel guiding mechanism with red membrane joints can be seen in Fig. 5. Other thickness accommodation techniques from origami design could be further adapted to DMs.

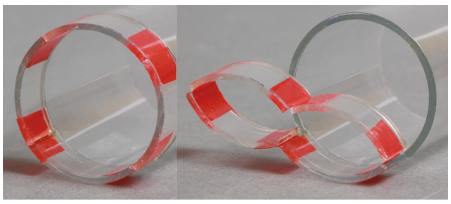

FIGURE 5. Parallel guiding cylindrical DM with membrane joints. The cylinder is 38 mm diameter polycarbonate tubing, cut on an Epilog M2 CO2 laser cutter, and the membrane is red acrylic tape.

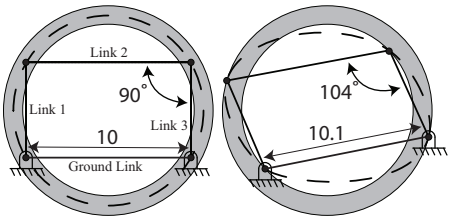

FIGURE 6. Left: Skeleton diagram showing a parallel guiding mechanism aligned to a reference surface (dotted line) in the middle of the cylinder walls. Right: The same parallel guiding mechanism, with the same link lengths, but with joints aligned with the inner or outer surface of the cylinder.

A second consideration is the shifting of the hinge position when using a membrane adhered to the inside or outside of the cylinder wall. This shifts the joint locations to the cylinder wall, which can change the reference surface and the link lengths. In the example shown in Fig. 6, links 1-3 are held at the same lengths, but the ground link has to change length if the joints are forced to the outside or inside of the cylinder wall. This may change the mechanism's classification and motion. In this example, the skeleton diagram of the linkage is no longer a cyclic quadrilateral [34] and the reference surface becomes a general cylinder.

3.5 Lamina Emergent Torsional (LET) joints

LET joints are created by removing specific sections from a planar material to enable a reduction of stiffness along a desired axis [35]. Many types of LET joints have been proposed and analyzed [20, 36–40]. These joints can allow for much greater deflections than simple single-beam compliant flexures of similar thickness due to the combination of multiple torsion and bending flexures in series and parallel. LET joints are promising for creating joint motion in cylindrical DMs because they allow large deflections and can be created from a plain cylinder by remov-

ing material. This can enable monolithic DMs. The adaptation of LET joints to curved surfaces was studied previously [23]. Equations were developed to determine the stiffness of a given curved LET joint. One example LET joint was analyzed analytically and compared to FEA results, with good agreement, at up to 20° of deflection. However, the joints analyzed were made from relatively thick walled material with large curvature.

A disadvantage mentioned for SLFPs also applies to LET joints: their center of rotation shifts during the deflection, resulting in the kinematic joint axes residing out of the reference surface. Existing LET joint models assume either a pure moment load or rotation displacement with no tensile or compressive forces. Likewise, the analysis in this work includes the assumption that the LET joints are loaded with a pure moment. Relatively thin-walled curved LET joints are analyzed here. It is expected that for a certain range of thickness-to-radius ratios, the equations used to analyze planar LET joints in [20] will also accurately predict joint stiffness in curved LET joints. This assumption would simplify the analysis of curved LET joints in relatively thin-walled cylindrical DMs.

4 MODELING CURVED LET JOINTS WITH THIN-WALLED ASSUMPTION

In [23], continuum mechanics equations (reported in [41]) are exploited to model the annular torsion sections created when cutting LET joints into a curved surface. The equation used to determine stiffness of the annular torsion beam contains a summation term. When using parameters for a LET joint in relatively thin-walled cylinders, the denominator in the summation term asymptotically approaches zero after a few iterations, causing the summation to reach infinity and therefore falsely return an infinite joint stiffness. This limitation motivated the assumption that the curved LET joints can be modeled as straight.

4.1 Evaluating the Thin-Walled Assumption

To validate further analysis, the torsional constant K of annular torsion beams at a specified range of thickness-to-radius ratios (t/R) was compared to the same property from square torsion beams with the same cross sectional area. For a torsion bar with circular cross section, K coincides with the polar moment of inertia, whereas for other sections K is to be evaluated resorting to numerical methods or, where available, with approximate formulations. In this work, the annular cross section constants were obtained in a FEA program (ANSYS). All other values were computed analytically, with square cross section constants being calculated using $K = 2.25a^4$ (taken from [42]), where a is half the length of one side of the square. Only the torsional constants were compared because the majority of deflection in a LET joint is due to twisting of the torsion beams. A visual comparison between the cross section with the largest t/R analyzed and a square beam of equal area is shown in Fig. 7, overlaid on a plot showing the error between the square and annular cross section torsion constants. The low error values demonstrated that further modeling may be fruitful.

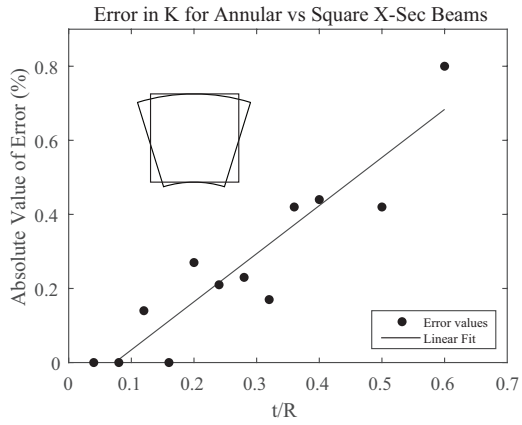

FIGURE 7. Plot showing relative error between torsional constants of annular cross section and rectangular cross section beams. The finite mesh used to obtain annular torsional constants may account for the non-smooth pattern from low to high t/R ratio.

The force deflection characteristic of the inside LET joint has been modeled by deriving the equivalent spring stiffness k_{eq} [20], such that $T = k_{eq}\theta$, where T is the total torque applied to the joint and θ is the joint angular deflection. Considering the analogous spring system depicted in Fig. 8(a), k_{eq} may be expressed as:

$$\frac{1}{k_{eq}} = \frac{1}{\frac{k_1 k_5}{k_1+k_5} + \frac{k_2 k_6}{k_2+k_6}} + \frac{1}{k_9} + \frac{1}{\frac{k_3 k_7}{k_3+k_7} + \frac{k_4 k_8}{k_4+k_8}} \tag{1}$$

where k_1, k_2, k_3 and k_4 represent the stiffness of the segments in torsion, and k_5, k_6, k_7, k_8 and k_9 are related to the segments in bending (see Fig. 8(b)). Each stiffness constant can be obtained by means of the following relations:

$$k_i = \frac{C_i G}{L_i}, \quad i = 1,..,4 \qquad k_i = \frac{EI_i}{L_i}, \quad i = 5,..,9 \tag{2}$$

where E is the modulus of elasticity, $G = E/2(1+\nu)$ is the shear modulus, L_i is the member's length (i.e. L_t for segments in torsion, L_b for segments in bending and L_c for the central member, as shown in Fig. 8(b)). C_i, namely a parameter analogous to the polar moment of inertia for circular cross sections, and I_i, namely

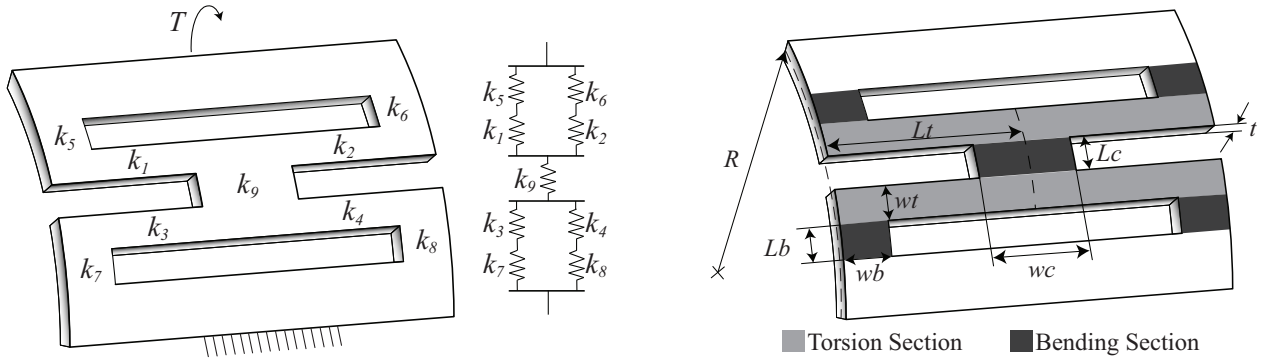

(a) Spring diagram for an inside LET joint.

(b) Principal dimensions for the inside LET joint.

FIGURE 8. Schematic describing parameters used in the Matlab analysis and elsewhere in this paper.

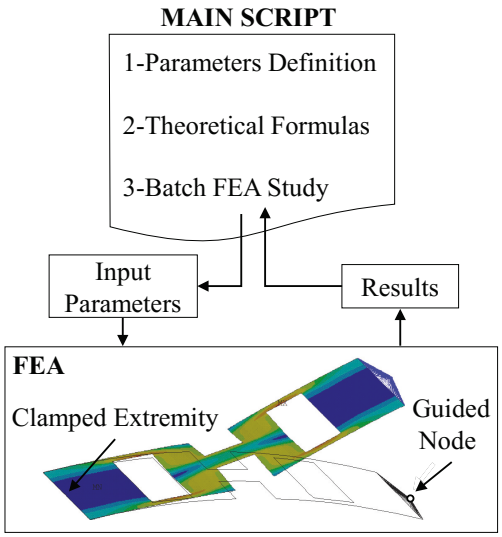

FIGURE 9. Schematic of the software framework.

the cross section's moment of inertia, are defined as [42]:

$$C_i = w_t t^3 \left[\frac{1}{3}\frac{64}{\pi^5}\frac{t}{w_t}\left(1-\frac{t^4}{12w_t^4}\right)\right], \quad i=1,..,4 \tag{3}$$

$$I_i = \frac{w_b t^3}{12}, \quad i=5,..,8 \tag{4}$$

$$I_i = \frac{w_c t^3}{12}, \quad i=9 \tag{5}$$

where w_t, w_b and w_c are the cross section's width and t is the LET thickness. A fast numerical routine aimed at validating the proposed theoretical models on the curved inside LET joint was created in a Matlab environment. The FEA program ANSYS

TABLE 1. LET parameters tested in the framework.

Param.	R	t	w_t	w_b
Value	5 mm	$[0.05, 0.25]$ mm	0.3 mm	0.3 mm
Param.	w_c	L_t	L_b	L_c
Value.	0.8 mm	1.25 mm	0.5 mm	0.5 mm

APDL and Matlab were combined in an integrated design framework [22] in which Matlab manages the parametric study, simulations, and the data exchange operations, as shown in Fig. 9. In this routine, ANSYS APDL provides the torque-deflection characteristic of each candidate via batch mode. The framework outputs the comparisons between theoretical and numerical results. Given w_t, w_b, w_c L_t, L_b, L_c, the behavior of the inside LET joint is investigated for several t/R values. Numerical values of each geometric parameter are presented in Tab. 1.

To perform the study, the following operations are addressed through a sequence of Matlab functions:

1. Creation of the design space and definition of N candidates.
2. Perform the theoretical calculations.
3. FEA batch simulations.
   For $i = 1$ to N
   - Update the ANSYS design parameter file with the i-th value ($(t/R)_i$);
   - Batch ANSYS Execution;
   - Import of the i-th results set

   End

Regarding the FEA models, a mapped mesh of Shell 181 ele-

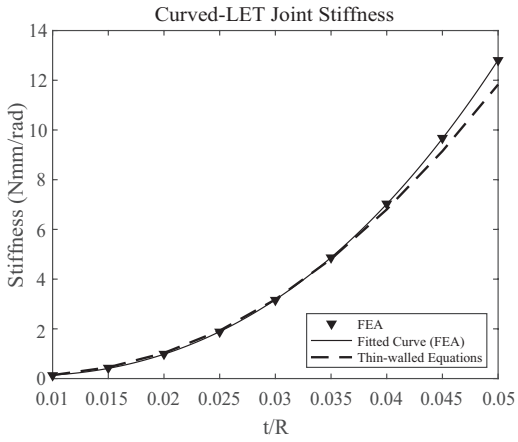

FIGURE 10. Curved LET joint stiffness comparison between FEA and thin-walled assumption models.

ments was defined for all the candidates. For boundary conditions, the LET joint is fully constrained at one extremity and guided in a pure rotation (35°) at the other. The material is Aluminum alloy 7075 (heat treated), with Young's modulus and Poisson's ratio of $E = 71.0$ GPa and $\nu = 0.334$, respectively. The achieved results, in terms of stiffness (i.e. k_{eq}), are reported in Fig. 10 for different values of t/R. From a direct comparison, the results obtained via FEA simulations show a good agreement with the behavior predicted by the theoretical formulations. As a consequence, planar equations can be used to design with acceptable accuracy curved LET joints for limited values of t/R.

4.2 Comparison of Thin-Walled LET Joint Prediction with Physical Prototype

To validate the analytical and FEA work, a small study was performed on the stiffness of 3D printed curved LET joints. To obtain an accurate bending modulus of elasticity of the printed material, sample flexion beams were printed on a Prusa i3 Mk2 in PETG with 100% infill and according to ASTM D790-03. These were tested in a 3-point bending setup using an Instron 3345 testing system. 3D printed PETG curved LET joints, with varying t/R ratios and a resultant bending modulus of $E = 1.4$ GPa, were then deflected using a guided rotation. The deflection path was obtained by exporting node locations from a LET joint in ANSYS with a pure moment applied. However, this path is not circular due to the joint's shifting axis of rotation. Due to the difficulty of applying a pure moment on a compliant joint with its axis shift, the path was approximated as circular for the medium angle of rotation being tested. The node locations from FEA were plotted. Under the assumption that the path was circular, a fixed point of rotation was approximated and a mounting system (see Fig. 11(a)) was designed to guide the LET joint through this approximated path.

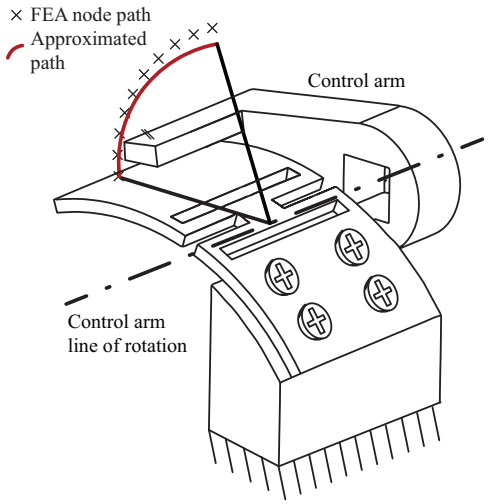

(a) Schematic showing the deflection path of the LET joint.

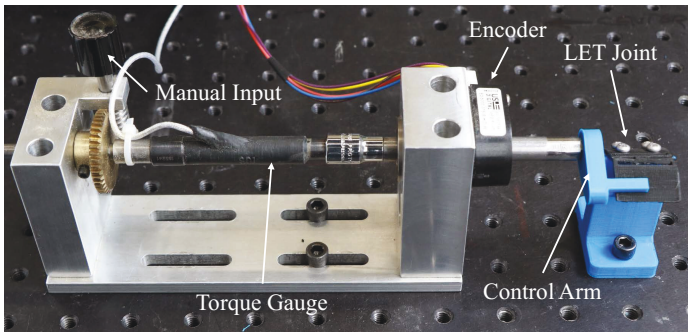

(b) Experimental setup.

FIGURE 11. Physical prototyping of the curved LET joint.

The deflection angle and torque applied was measured using a US Digital E2-5000-375 laser encoder (resolution of +/-0.07°) and the Omega TQ103-50 torque gauge, respectively. The test setup is shown in Fig. 11. Due to the slow manual actuation and the unidirectional testing to obtain the stiffness of the LET joints, hysteresis in the torque gauge was not seen in the test results. These results are plotted in Fig. 12, where the 3D printed joint stiffness is compared to the stiffness obtained by both planar LET joint equations and the FEA model. The physical data are in good agreement with the FEA results considering the inherent variability of material properties and dimensions with fused deposition 3D printing. Using FEA as the reference behavior, the discrepancy between predicted and measured data has a median error of 14%. In addition to fabrication variability, the differences may be attributed to the circular path assumption in the test setup (see Fig. 11(a)) and to the slight unevenness of the manual deflection of the LET joints.

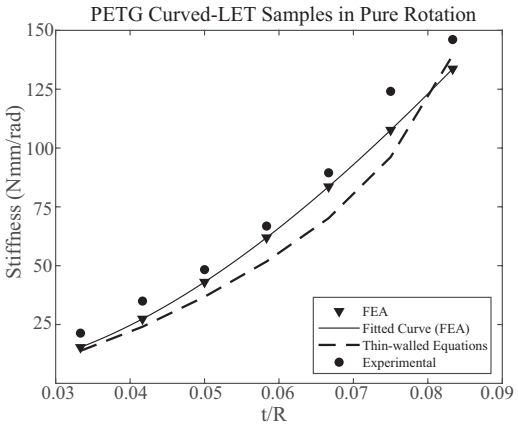

FIGURE 12. Comparison of experimentally derived 3D printed curved LET joint stiffness to FEA and thin-walled LET models.

4.3 Discussion on LET Joints

LET joints show promise for application in cylindrical DMs due to their ability to enable relatively large hinge motion using only the material in the cylinder itself. The analysis performed validated the use of the proposed equations for LET joints in thin-walled cylinders, which could improve efficiency on curved LET joint design. While LET joints enable larger deflections than other compliant joints, a quick analysis using the Matlab routine in Section 4 showed that a single curved LET joint cut into a metal (steel, aluminum, or titanium) thin-walled cylinder will plastically deform before reaching the large deflections ($\theta > 40^\circ$) required in some cylindrical DMs. It is also important to reiterate that the models analyzed in this work assume a pure moment or rotation is applied to the LET joint, yet compliant joints in kinematic mechanisms are subjected to combined loads.

5 AT-SCALE LAPAROSCOPIC SURGICAL DEVICE IN NITINOL

A cylindrical DM was discussed and designed in [13] for being used as an end-effector in minimally invasive or laparoscopic surgery. End-effectors are specialized tools at the end of laparoscopic shafts designed to manipulate body tissue in a specific way. It was desired to analyze the same device, shown in Fig. 13 and termed the multiplying cylinder, with LET joints at a scale comparable to laparoscopic surgical devices on the market. This would mean embedding LET joints into a cylinder that is 5 mm in diameter with a wall thickness of less than 0.5 mm. Using LET joints to achieve the large deflections required in the multiplying cylinder device at this scale may require the use of exotic materials.

In the multiplying cylinder device, an outer cylinder with two joints fits over an inner cylinder that attaches to the end of one of the links. The inner cylinder is then rotated with respect to the outer to actuate the device. Between the stowed and deployed state, one of the joints in this device travels through 90° of deflection. Preliminary analysis using the routine from Section 4 showed that a single LET joint, in conventional metals and at the desired scale, could not accomplish this deflection. It was therefore decided to model the device with superelastic Nitinol. Nitinol has a unique, non-linear stress-strain curve. Therefore, the at-scale model could not be analyzed in Nitinol using the analysis method from Section 4, which requires the definition of E and ν. To accomplish this task, a model of the expanding cylinder mechanism, with the dimensions in Tab. 2, was analyzed in ANSYS with a multi-linear stress-strain curve to match the behavior reported in a previous study on superelastic Nitinol under

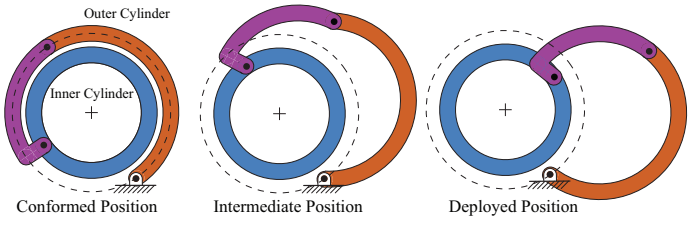

FIGURE 13. Functional schematic of the multiplying cylinder mechanism.

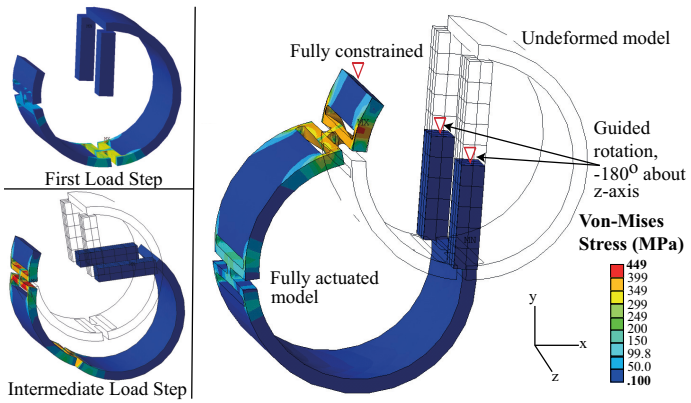

FIGURE 14. FEA results of the Expanding Cylinder mechanisms with LET joints in Nitinol.

TABLE 2. Dimensions of Nitinol LET model.

Param.	R	t	w_t	w_b
Value	5 mm	0.3 mm	0.2 mm	0.2 mm
Param.	w_c	L_t	L_b	L_c
Value.	0.4 mm	2 mm	0.2 mm	0.2 mm

biaxial loading [43]. Solid187 elements were used with a tetrahedral mesh that was refined at each LET joint. The rectangular sections were modeled as perfectly rigid and used to replicate the cylinder-in-cylinder actuation of the original device. Each device was actuated to full deployment, which involves rotating the "inner cylinder" 180°, resulting in 90° of deflection in one of the LET joints. The model shown in Fig. 14 reached a maximum Von Mises stress of 449 MPa and a maximum strain of 0.0483. While reported material properties for superelastic Nitinol vary widely, the strain and stress values are unlikely to cause yielding [44]. This model suggests that LET joints cut into a Nitinol cylinder could enable cylindrical DMs to exist in the laparoscopic surgery market.

6 CONCLUSIONS

In this work, possible options for hinges in cylindrical DMs were reviewed and analyzed. Classical methods such as pin hinges are difficult due to manufacturing and loading concerns when reaching small scale parts. Simple compliant joints, such as SLFPs, can be useful for large curvature joints but suffer from modeling issues due to the combined loadings. Membrane joints show promise for small-scale mechanisms due to their simplicity, but the joint axis must shift to the outside or inside of the cylinder wall, which changes the initial or closed position of the mechanism if all link lengths are held the same. LET joints may be advantageous in cylindrical DMs due to the large deflections often reached.

A Matlab and ANSYS integrated routine was developed to compare planar LET joint stiffness models developed previously to curved LET joint FEA models. For curved LET joints cut from thin-walled cylinders with a thickness-to-radius ratio of 0.032 to 0.08, there is good agreement between the simplified models and the curved FEA models. This suggests the previously developed non-curved models are sufficient for curved LET joints in this range. The analytical and numerical models were also compared to 3D printed curved LET joints, and these results also showed good agreement. Finally, a cylinder-in-cylinder actuated cylindrical DM was modeled in FEA in Nitinol, with dimensions similar to those seen in laparoscopic surgical tools. This model showed that LET joints may be suitable for medical device applications where exotic materials such as Nitinol are more commonly found.

FUNDING SOURCES

This material is based on work supported by the National Science Foundation under grant NSF-1663345.

REFERENCES

[1] Nelson, T. G., Zimmerman, T. K., Magleby, S. P., Lang, R. J., and Howell, L. L., 2019. "Developable mechanisms on developable surfaces". *Science Robotics,* ***4***(27).

[2] Nelson, T. G., and Herder, J. L., 2018. "Developable compliant-aided rolling-contact mechanisms". *Mechanism and Machine Theory,* ***126***, pp. 225–242.

[3] Jacobsen, J. O., Winder, B. G., Howell, L. L., and Magleby, S. P., 2010. "Lamina emergent mechanisms and their basic elements". *Journal of Mechanisms and Robotics,* ***2***(1).

[4] Greenwood, J. R., Magleby, S. P., and Howell, L. L., 2019. "Developable mechanisms on regular cylindrical surfaces". *Mechanism and Machine Theory,* ***142***, p. 103584.

[5] Peyron, Q., Rabenorosoa, K., Andreff, N., and Renaud, P., 2019. "A numerical framework for the stability and cardinality analysis of concentric tube robots: Introduction and application to the follow-the-leader deployment". *Mechanism and Machine Theory,* ***132***, pp. 176–192.

[6] Venkiteswaran, V. K., Sikorski, J., and Misra, S., 2019. "Shape and contact force estimation of continuum manipulators using pseudo rigid body models". *Mechanism and Machine theory,* ***139***, pp. 34–45.

[7] Lim, J. J., and Erdman, A. G., 2003. "A review of mechanism used in laparoscopic surgical instruments". *Mechanism and Machine Theory,* ***38***(11), pp. 1133–1147.

[8] Xue, R., Du, Z., Yan, Z., and Ren, B., 2019. "An estimation method of grasping force for laparoscope surgical robot based on the model of a cable-pulley system". *Mechanism and Machine Theory,* ***134***, pp. 440–454.

[9] Chang, J., Boules, M., Rodriguez, J., and Kroh, M., 2016. "Minilaparoscopy with interchangeable, Full 5-mm end effectors: First human use of a new minimally invasive operating platform". *Journal of Laparoendoscopic and Advanced Surgical Techniques and Videoscopy,* ***26***(1), pp. 1–5.

[10] Zoppi, M., Sieklicki, W., and Molfino, R., 2008. "Design of a microrobotic wrist for needle laparoscopic surgery". *Journal of Mechanical Design,* ***130***(10).

[11] Gafford, J., Ding, Y., Harris, A., McKenna, T., Polygerinos, P., Holland, D., Walsh, C., and Moser, A., 2015. "Shape deposition manufacturing of a soft, atraumatic, and deployable surgical grasper". *Journal of Mechanisms and Robotics,* ***7***(2).

[12] Howell, L. L., 2001. *Compliant mechanisms*. John Wiley & Sons.

[13] Seymour, K., Sheffield, J., Magleby, S. P., and Howell, L. L., 2019. "Cylindrical developable mechanisms for minimally invasive surgical instruments". *ASME IDETC/CIE International Design Engineering Technical Conferences and Computers and Information in Engineering Conference*.

[14] Megaro, V., Zehnder, J., Bächer, M., Coros, S., Gross,

M. H., and Thomaszewski, B., 2017. "A computational design tool for compliant mechanisms". *ACM Transactions on Graphics,* ***36***, pp. 82:1–82:12.

[15] Su, H., 2009. "A pseudorigid-body 3R model for determining large deflection of cantilever beams subject to tip loads". *Journal of Mechanisms and Robotics,* ***1***(2).

[16] Pedersen, C., Buhl, T., and Sigmund, O., 2001. "Topology synthesis of large-displacement compliant mechanisms". *International Journal for Numerical Methods in Engineering,* ***50***(12), pp. 2683–2705.

[17] Sigmund, O., 1997. "On the design of compliant mechanisms using topology optimization". *Mechanics of Structures and Machines,* ***25***(4), pp. 493–524.

[18] Aten, Q. T., Jensen, B. D., Tamowski, S., Wilson, A. M., Howell, L. L., and Burnett, S. H., 2012. "Nanoinjection: pronuclear DNA delivery using a charged lance". *Transgenic Research,* ***21***(6), pp. 1279–1290.

[19] Last, M., Subramaniam, V., and Pister, K., 2012. "Out-of-plane motion of assembled microstructures using a single-mask SOI process". *IEEE 13th International Conference on Solid-State Sensors, Actuators, and Microsystems,* ***2***.

[20] Jacobsen, J., Chen, G., Howell, L., and Magleby, S., 2012. "Lamina emergent torsional (LET) joint". *Mechanism and Machine Theory,* ***56***, pp. 1–15.

[21] Nelson, T. G., Lang, R. J., Pehrson, N. A., Magleby, S. P., and Howell, L. L., 2016. "Facilitating deployable mechanisms and structures via developable lamina emergent arrays". *Journal of Mechanisms and Robotics,* ***8***(3).

[22] Pehrson, N. A., Bilancia, P., Magleby, S., and Howell, L., 2020. "Load–displacement characterization in three degrees-of-freedom for general lamina emergent torsion arrays". *Journal of Mechanical Design,* ***142***(9).

[23] Zimmerman, T., Butler, J., Frandsen, D., Burrow, D., Fullwood, D., Magleby, S., and Howell, L., 2018. "Modified material properties in curved panels through lamina emergent torsional joints". *ReMAR International Conference on Reconfigurable Mechanisms and Robots*, pp. 1–9.

[24] Hwang, I.-H., Shim, Y.-S., and Lee, J.-H., 2003. "Modeling and experimental characterization of the chevron-type bi-stable microactuator". *Journal of Micromechanics and Microengineering,* ***13***(6), pp. 948–954.

[25] Ferreira, H., 2015. "Equipment in laparoscopic surgery". *A manual of minimally invasive gynecological surgery*, pp. 3–12.

[26] Li, L., Zhang, D., Guo, S., and Qu, H., 2019. "Design, modeling, and analysis of hybrid flexure hinges". *Mechanism and Machine Theory,* ***131***, pp. 300–316.

[27] Linß, S., Gräser, P., Räder, T., Henning, S., Theska, R., and Zentner, L., 2018. "Influence of geometric scaling on the elasto-kinematic properties of flexure hinges and compliant mechanisms". *Mechanism and Machine Theory,* ***125***, pp. 220–239.

[28] Midha, A., and Kuber, R., 2014. "Closed-form elliptic integral solution of initially-straight and initially-curved small-length flexural pivots". *ASME IDETC/CIE International Design Engineering Technical Conferences and Computers and Information in Engineering Conference*.

[29] Howell, L. L., Midha, A., and Norton, T., 1996. "Evaluation of equivalent spring stiffness for use in a pseudo-rigid-body model of large-deflection compliant mechanisms". *Journal of Mechanical Design,* ***118***(1), pp. 126–131.

[30] Lang, R. J., Tolman, K. A., Crampton, E. B., Magleby, S. P., and Howell, L. L., 2018. "A review of thickness-accommodation techniques in origami-inspired engineering". *Applied Mechanics Reviews,* ***70***(1).

[31] Zirbel, S. A., Lang, R. J., Thomson, M. W., Sigel, D. A., Walkemeyer, P. E., Trease, B. P., Magleby, S. P., and Howell, L. L., 2013. "Accommodating thickness in origami-based deployable arrays". *Journal of Mechanical Design,* ***135***(11).

[32] Chen, G., Magleby, S. P., and Howell, L. L., 2018. "Membrane-enhanced lamina emergent torsional joints for surrogate folds". *Journal of Mechanical Design,* ***140***(6).

[33] Seymour, K., Burrow, D., Avila, A., Bateman, T., Morgan, D. C., Magleby, S. P., and Howell, L. L., 2018. "Origami-based deployable ballistic barrier". *7OSME 7th International Meeting on Origami in Science, Mathematics and Education*, pp. 763–777.

[34] Villiers, M. D., 1994. "The role and function of a hierarchical classification of quadrilaterals". *For the Learning of Mathematics,* ***14***(1), pp. 11–18.

[35] DeFigueiredo, B. P., Zimmerman, T. K., Russell, B. D., and Howell, L. L., 2018. "Regional stiffness reduction using lamina emergent torsional joints for flexible printed circuit board design". *Journal of Electronic Packaging,* ***140***(4), p. 041001.

[36] Xie, Z., Qiu, L., and Yang, D., 2018. "Using the parts used to be removed to improve compliant joint's performance". *ASME IDETC/CIE International Design Engineering Technical Conferences and Computers and Information in Engineering Conference*.

[37] Klett, Y., 2018. "PALEO: Plastically annealed lamina emergent origami". *ASME IDETC/CIE International Design Engineering Technical Conferences and Computers and Information in Engineering Conference*.

[38] Alfattani, R., and Lusk, C., 2016. "A lamina-emergent frustum using a bistable collapsible compliant mechanism (BCCM)". *ASME IDETC/CIE International Design Engineering Technical Conferences and Computers and Information in Engineering Conference*.

[39] Xie, Z., Qiu, L., and Yang, D., 2017. "Design and analysis of outside-deployed lamina emergent joint (OD-LEJ)". *Mechanism and Machine Theory,* ***114***, pp. 111–124.

[40] Xie, Z., Qiu, L., and Yang, D., 2018. "Design and analy-

sis of a variable stiffness inside-deployed lamina emergent joint". *Mechanism and Machine Theory,* ***120***, pp. 166–177.
[41] Jog, C., 2015. *Continuum Mechanics: Foundations and Applications of Mechanics, Volume I, 2015*, 3rd ed., Vol. 1. Cambridge University Press.
[42] Roark, R. J., and Young, W. C., 1975. *Formulas for stress and strain*. McGraw-Hill.
[43] McNaney, J., Imbeni, V., Jung, Y., Papadopoulos, P., and Ritchie, R., 2003. "An experimental study of the superelastic effect in a shape-memory nitinol alloy under biaxial loading". *Mechanics of Materials,* ***35***(10), pp. 969 – 986.
[44] Qian, H., Li, H., Song, G., and Guo, W., 2013. "Recentering shape memory alloy passive damper for structural vibration control". *Mathematical Problems in Engineering,* ***2013***, pp. 1–13.